Journal of Theoretical Biology 548 (2022) 111195

Contents lists available at ScienceDirect

Journal of Theoretical Biology

journal homepage: www.elsevier.com/locate/yjtbi

A direct comparison of methods for assessing the threat from emerging infectious diseases in seasonally varying environments

A.R. Kaye [a,b], W.S. Hart [c], J. Bromiley [c], S. Iwami [d], R.N. Thompson [a,b,*]

[a] Mathematics Institute, University of Warwick, Coventry, UK
[b] Zeeman Institute for Systems Biology and Infectious Disease Epidemiology Research, University of Warwick, Coventry, UK
[c] Mathematical Institute, University of Oxford, Oxford, UK
[d] Department of Biology, Nagoya University, Nagoya, Japan

ARTICLE INFO

Article history:
Received 8 November 2021
Revised 4 May 2022
Accepted 6 June 2022
Available online 16 June 2022

Keywords:
Mathematical modelling
Infectious disease epidemiology
Major epidemic
Seasonal variability
Host-vector model

ABSTRACT

Seasonal variations in environmental conditions lead to changing infectious disease epidemic risks at different times of year. The probability that early cases initiate a major epidemic depends on the season in which the pathogen enters the population. The instantaneous epidemic risk (IER) can be tracked. This quantity is straightforward to calculate, and corresponds to the probability of a major epidemic starting from a single case introduced at time $t = t_0$, assuming that environmental conditions remain identical from that time onwards (i.e. for all $t \geq t_0$). However, the threat when a pathogen enters the population in fact depends on changes in environmental conditions occurring within the timescale of the initial phase of the outbreak. For that reason, we compare the IER with a different metric: the case epidemic risk (CER). The CER corresponds to the probability of a major epidemic starting from a single case entering the population at time $t = t_0$, accounting for changes in environmental conditions after that time. We show how the IER and CER can be calculated using different epidemiological models (the stochastic Susceptible-Infectious-Removed model and a stochastic host-vector model that is parameterised using temperature data for Miami) in which transmission parameter values vary temporally. While the IER is always easy to calculate numerically, the adaptable method we provide for calculating the CER for the host-vector model can also be applied easily and solved using widely available software tools. In line with previous research, we demonstrate that, if a pathogen is likely to either invade the population or fade out on a fast timescale compared to changes in environmental conditions, the IER closely matches the CER. However, if this is not the case, the IER and the CER can be significantly different, and so the CER should be used. This demonstrates the need to consider future changes in environmental conditions carefully when assessing the risk posed by emerging pathogens.

1. Introduction

Pathogens can be introduced into host populations in different ways, including zoonotic spillover (Plowright et al., 2017; Borremans et al., 2019; Lloyd-Smith et al., 2009; Nandi and Allen, 2021) and importation from other locations (Daon et al., 2020; Thompson et al., 2019b; Wilson, 1995). However, when a pathogen enters a population, a major epidemic does not always follow. The pathogen may establish in the population and cause a major epidemic with a large number of cases, or instead fade out as a minor outbreak with few cases (Craft et al., 2013; Lovell-Read et al., 2021; Thompson et al., 2016). Environmental conditions play a significant role in the epidemic risk when pathogen introduction occurs. Weather and climate factors are known to affect pathogen survival ability (Shaman and Kohn, 2009; Tang, 2009) and host immune responses (Dowell, 2001; Moriyama and Ichinohe, 2019). Furthermore, the transmission of vector-borne pathogens is affected by variables such as temperature, precipitation and humidity, which can alter the lifespans and flight distances of vectors (Yang et al., 2009; Rowley and Graham, 1968), among other characteristics. Environmental changes, in addition to factors such as changes in host behaviour, lead to epidemic risks that vary during the year (Grassly and Fraser, 2006).

Models that do not account for temporal variations in environmental conditions are now used routinely for a range of diseases to assess the risk that initial cases will lead to a major epidemic (Fig. S1), often by assuming that infections occur according to a branching process (Althaus et al., 2015; Hellewell et al., 2020;

* Corresponding author at: Mathematics Institute, University of Warwick, Coventry, UK.
E-mail address: robin.n.thompson@warwick.ac.uk (R.N. Thompson).

https://doi.org/10.1016/j.jtbi.2022.111195
0022-5193/

Thompson, 2020). Such approaches can be applied in the context of epidemiological models in which pathogen transmission parameters vary temporally by inferring the epidemic risk based on the parameter values at the precise instant that the pathogen enters the host population (Guzzetta et al., 2016a,b; Thompson et al., 2020b). Since the epidemic risk estimated in this way depends only on the environmental conditions at the time of pathogen introduction, rather than the future environmental conditions and changes in other factors affecting transmission (which may be unknown at that time), this straightforward approach can be applied to approximate epidemic risks in real-time at the beginning of a potential epidemic.

However, in scenarios in which environmental conditions change relatively predictably, such as seasonal changes in weather, then future changes in environmental conditions are known and can be included in epidemic risk calculations. In the 1940s, Kendall (1948) showed how the probability that a birth-and-death process will go extinct starting from a single individual can be calculated while accounting for periodic birth and death rates. This work led to a range of analyses exploring the impact of seasonality on ecological invasion probabilities and epidemiological extinction probabilities (Nipa and Allen, 2020; Ball, 1983; Bacaër and Ait Dads, 2014; Bacaër and Ed-Darraz, 2014). Recently, studies by Bacaër (2020a,b) and Carmona and Gandon (2020) have compared epidemic risks (or ecological invasion probabilities) calculated in the "naïve" way (based only on environmental conditions when the pathogen enters the population) with those including future changes in environmental conditions. Carmona and Gandon (2020) demonstrated that the epidemic risk when a pathogen enters the population may be lower than expected if environmental conditions will become less suitable for transmission in the near future. That work highlighted that epidemic risk calculations based on both current and future values of transmission parameters should receive more attention, particularly in the applied epidemiological modelling literature.

Here, we define two metrics for quantifying the epidemic risk in the initial stages of an outbreak: the instantaneous epidemic risk (IER) and the case epidemic risk (CER). The names of the IER and CER are inspired by two different versions of the time-dependent reproduction number (the instantaneous reproduction number and case reproduction number (Abbott et al., 2020; Cori et al., 2013; Gostic et al., 2020; Thompson et al., 2019a; White et al., 2020)), a measure of pathogen transmissibility that can be tracked in real-time after a pathogen has successfully invaded a host population. The instantaneous reproduction number describes pathogen transmissibility at the exact time under consideration, whereas the case reproduction number accounts for changes in pathogen transmission that occur in the near future. Similarly, the IER considered here is defined to be the probability of a major epidemic starting from a single case entering the population at time $t = t_0$, assuming that environmental conditions remain identical from then onwards. The CER also represents the probability of a major epidemic starting from a single case entering the population at time $t = t_0$, but instead accounts for changes in environmental conditions that occur after that time. We compare epidemic risks calculated using: i) branching process approximations of the stochastic compartmental models considered (see below); ii) stochastic simulations of the full compartmental models, in which we differentiate "major epidemics" from "minor outbreaks" based on the total number of infections in the outbreak (i.e., a major epidemic is defined as an outbreak in which a pre-defined threshold number of infections is exceeded; the CER at time $t = t_0$ is then the proportion of simulations starting from a single case that are major epidemics). We verify that these approaches both generate similar results. Although the terms "IER" and "CER" are new, these quantities were considered in the literature described above (for example, the CER is analogous to the "emergence probability" considered by Carmona and Gandon (2020), and the CER for the stochastic Susceptible-Infectious-Removed (SIR) model is equivalent to the expression derived for birth-and-death processes by Kendall (1948)). We extend the method used by Carmona and Gandon (2020) and provide an easy-to-use framework for deriving and solving differential equations satisfied by the CER numerically for a wide range of epidemiological models.

To demonstrate the extensibility of our methods, we consider two models: (i) the stochastic SIR model; (ii) a stochastic host-vector model that includes a temperature-dependent vector lifespan that we parameterise using temperature data from Miami. We then compare risk assessments made using the IER and CER directly. If a pathogen either fades out or invades a population quickly compared to changes in environmental conditions, then the IER provides an easy-to-calculate and accurate estimate of the risk from the invading pathogen. However, if the initial stage of the outbreak occurs over a longer timescale, then the epidemic risk can be significantly different to that predicted by the IER. In those cases, it is necessary to use the CER. This shows that it can be essential to account for future changes in environmental conditions carefully when assessing the risk posed by emerging pathogens.

2. Methods

2.1. Models

2.1.1. SIR model

The deterministic SIR model with time-dependent infection and removal rates is:

$$\frac{\mathrm{d}S(t)}{\mathrm{d}t} = -\frac{\beta(t)S(t)I(t)}{N}, \frac{\mathrm{d}I(t)}{\mathrm{d}t} = \frac{\beta(t)S(t)I(t)}{N} - \mu(t)I(t),$$
$$\frac{\mathrm{d}R(t)}{\mathrm{d}t} = \mu(t)I(t). \tag{1}$$

In this model, $S(t)$ is the number of individuals who are susceptible to the pathogen at time t, $I(t)$ is the number infected and infectious, and $R(t)$ is the number removed (recovered or dead). The total population size, $S(t) + I(t) + R(t) = N$, is assumed to be constant. We consider the analogous stochastic model, and run simulations using a modified version of the Gillespie direct method (Gillespie, 1977) in which time-dependent rate parameters are accounted for (Mastin et al., 2020; Thanh and Priami, 2015) (Text S1).

In our analyses, time t is measured in months and the infection rate is chosen to be periodic with period 12 months:

$$\beta(t) = \beta_0 + \beta_1 \cos\left(\frac{\pi}{6}t - \varphi\right), \tag{2}$$

where $\beta_0 > \beta_1$. The removal rate is assumed to be constant ($\mu(t) = \mu$). Although we use these parameter choices to demonstrate our approach, expressions for the IER and CER are derived for general periodic functions $\beta(t)$ and $\mu(t)$. Parameter values used are shown in the captions to Figs. 1 and 2.

2.1.2. Host-vector model

We also consider a host-vector model:

$$\begin{aligned}
\tfrac{\mathrm{d}S(t)}{\mathrm{d}t} &= -\tfrac{\beta(t)I^V(t)S(t)}{N}, \ \tfrac{\mathrm{d}E(t)}{\mathrm{d}t} = \tfrac{\beta(t)I^V(t)S(t)}{N} - \alpha(t)E(t),\\
\tfrac{\mathrm{d}I(t)}{\mathrm{d}t} &= \alpha(t)E(t) - \mu(t)I(t), \ \tfrac{\mathrm{d}R(t)}{\mathrm{d}t} = \mu(t)I(t),\\
\tfrac{\mathrm{d}S^V(t)}{\mathrm{d}t} &= \delta(t)N^V - \tfrac{\beta_V(t)S^V(t)I(t)}{N} - \delta(t)S^V(t),\\
\tfrac{\mathrm{d}E^V(t)}{\mathrm{d}t} &= \tfrac{\beta_V(t)S^V(t)I(t)}{N} - (\delta(t) + \alpha_V(t))E^V(t),\\
\tfrac{\mathrm{d}I^V(t)}{\mathrm{d}t} &= \alpha_V(t)E^V(t) - \delta(t)I^V(t).
\end{aligned} \tag{3}$$

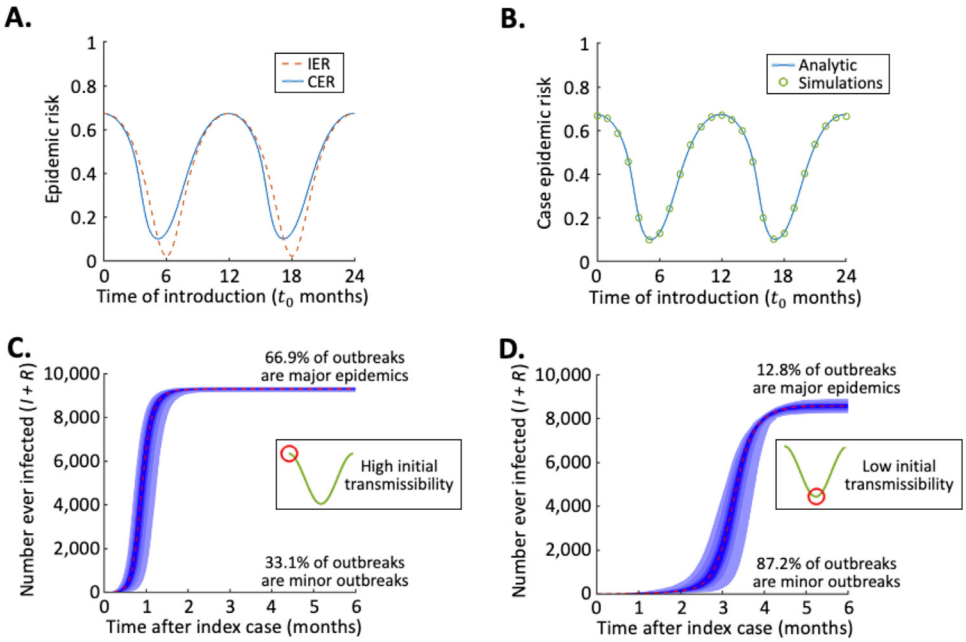

Fig. 1. The IER and CER for the SIR model. A. The IER (Eq. (5); red dotted) and CER (Eq. (9); blue) can be calculated to assess the probability of a major epidemic when a pathogen first arrives in a new host population. B. The CER can either be calculated numerically using Eq. (9) (blue) or approximated using model simulations (Text S1; green circles). C. Simulations of the SIR model (Text S1) when the pathogen arrives in the population when environmental conditions are (instantaneously) most appropriate for pathogen transmission ($t_0 = 0$ months). D. Analogous results to C when the pathogen arrives in the population when environmental conditions are (instantaneously) least appropriate for pathogen transmission ($t_0 = 6$ months). In panel B, simulation results were obtained using 10,000 model simulations for each CER value shown. In panels C and D, the blue shaded region represents the 95% credible interval of 10,000 simulated major epidemics, where the time on the x-axis represents the number of months after the pathogen arrives in the population. In the simulation results in panels B-D, major epidemics were classified as outbreaks in which at least 1,000 individuals were infected during the outbreak. In all panels, $\beta(t)$ is given by Eq. (2) and $\mu(t)$ is assumed to take a constant value ($\mu(t) = \mu$). Parameter values: $N = 10{,}000$, $\beta_0 = 10$ month^{-1}, $\beta_1 = 5$ month^{-1}, $\varphi = 0$, $\mu = 4.9$ month^{-1} (so that $\beta(t)/\mu$, which would be the instantaneous reproduction number if a single case arrived in the population at time t, varies between 1.02 and 3.06 at different times of year). (For interpretation of the references to colour in this figure legend, the reader is referred to the web version of this article.)

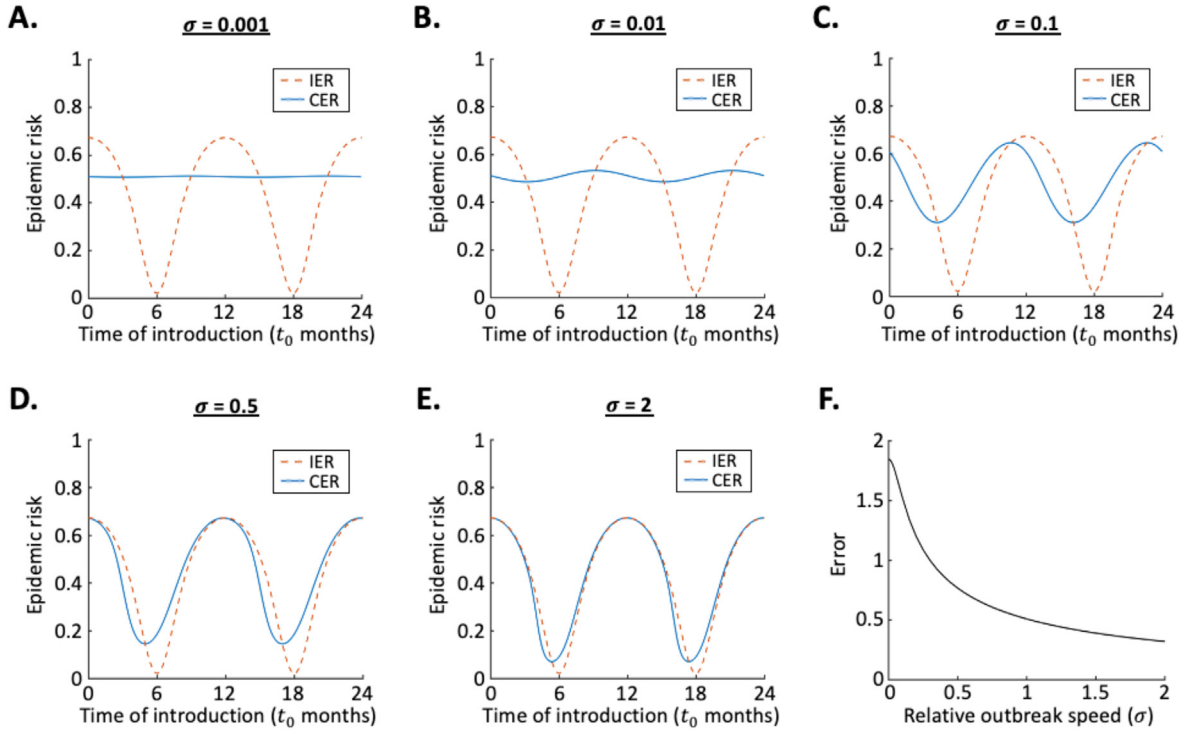

Fig. 2. Comparing the IER and CER for the SIR model for outbreaks of different speeds. A. The IER (Eq. (5); red dotted) and CER (Eq. (9); blue) when the outbreak speed is slow ($\sigma = 0.001$). B-E. Analogous figures to A, but with $\sigma = 0.01$ (panel B), $\sigma = 0.1$ (panel C), $\sigma = 0.5$ (panel D) and $\sigma = 2$ (panel E). F. The error between the IER and CER, computed as $\frac{\int_0^{12} |\mathrm{CER}(t_0) - \mathrm{IER}(t_0)| \mathrm{d}t_0}{\int_0^{12} \mathrm{CER}(t_0) \mathrm{d}t_0}$, as a function of the relative outbreak speed (σ). Parameter values: $N = 10{,}000$, $\beta_0 = 10$ month^{-1}, $\beta_1 = 5$ month^{-1}, $\varphi = 0$, $\mu = 4.9$ month^{-1} (so that, as in Fig. 1, $\beta(t)/\mu$ varies between 1.02 and 3.06 at different times of year). To vary the speed of the outbreak in each panel, the values of β_0, β_1 and μ are all multiplied by the relevant value of σ. (For interpretation of the references to colour in this figure legend, the reader is referred to the web version of this article.)

In this model, the total host population size $(S(t)+E(t)+I(t)+R(t)=N)$ and the total vector population size $(S^V(t)+E^V(t)+I^V(t)=N^V)$ are both constant. The parameters $\beta(t)$ and $\beta_V(t)$ govern the rates at which infectious vectors infect susceptible hosts and susceptible vectors acquire the pathogen from infectious hosts, respectively. Exposed hosts and vectors become infectious at rates $\alpha(t)$ and $\alpha_V(t)$. The parameter $\mu(t)$ is the removal rate of infectious hosts, and $\delta(t)$ describes the mortality rate of every vector (where dead vectors are replaced by new susceptible vectors). We again consider the analogous stochastic model, simulated using a modified version of the Gillespie direct method (Mastin et al., 2020; Thanh and Priami, 2015) (Text S1).

In our analyses, we assume that the vector mortality rate varies temporally due to seasonal temperature variations. Specifically, the temperature $\tau(t)$ is assumed to vary with period 12 months:

$$\tau(t)=\tau_0+\tau_1\cos\left(\frac{\pi}{6}t-\gamma\right). \tag{4}$$

The values of the parameters τ_0, τ_1 and γ were determined by fitting $\tau(t)$ to monthly mean temperature data from Miami from 2018 to 2019 (Data S1 – obtained from National Oceanic and Atmospheric Administration (2020)) using least squares estimation, with time $t=0$ months corresponding to 1st January 2018.

As estimated from laboratory experiments in adult female *Aedes aegypti* mosquitoes by Yang et al. (2009), the vector mortality rate is assumed to depend on the temperature according to the quartic polynomial $\delta(t)=\sum_{i=0}^{4} b_i\tau(t)^i$, where $b_0=26.4$ month^{-1}, $b_1=-4.84$ month^{-1} °C^{-1}, $b_2=0.339$ month^{-1} °C^{-2}, $b_3=-0.0104$ month^{-1} °C^{-3} and $b_4=0.000116$ month^{-1} °C^{-4}. These values have been rescaled from the daily rates in the original publication (Yang et al., 2009) to monthly rates, for consistency with the temperature data.

In our analyses, we consider the effect of temperature on the vector lifespan, and therefore on the IER and CER. To consider this effect alone, we assume that parameters other than the vector mortality rate take constant values; parameter values are shown in the caption to Fig. 3. The main purpose of this research is to explore general differences between the IER and CER, and to provide an extensible framework for their calculation, rather than to predict epidemic risks precisely for a specific pathogen in a particular location. However, to ensure that the assumed parameter values remain realistic, we take these values, where possible, from a study of Zika virus transmission by Kucharski et al. (2016), adjusted to the appropriate monthly rates. Nonetheless, the IER and CER are again derived generally.

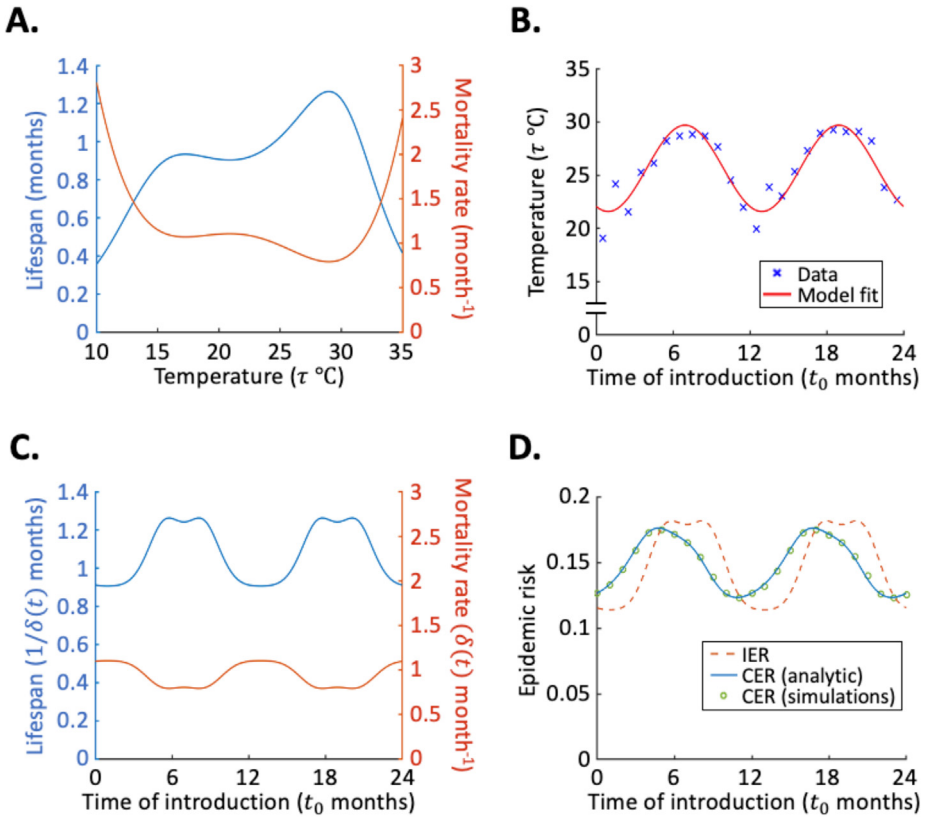

Fig. 3. The impact of seasonal changes in environmental conditions on the IER and CER for the host-vector model. A. Assumed dependence of the vector lifespan (blue) and mortality rate (red) on temperature, derived from laboratory experiments in adult female *Aedes aegypti* mosquitoes (Yang et al., 2009). B. Temperature in Miami from 2018 to 2019 (red; Eq. (4)) fitted to data (blue stars; obtained from National Oceanic and Atmospheric Administration (2020)) using least squares estimation; best fit parameters are $\tau_0=25.7$ °C, $\tau_1=-4.07$ °C and $\gamma=0.490$. C. Inferred vector lifespan and mortality rate based on the relationships in panels A and B. D. The IER (Eq. (6); red dotted), CER calculated numerically (system of equations (10); blue) and CER calculated using model simulations (Text S1; green circles) for the host-vector model (analogous stochastic model to system of equations (3)). In panel D, simulation results were obtained using 10,000 model simulations for each CER value shown, with major epidemics classified as outbreaks in which at least 1,000 hosts became infected during the outbreak. Parameters other than the vector mortality rate ($\delta(t)$, which varies as shown in panel C) were assumed constant (so that e.g. $\beta(t)=\beta$). Parameter values: $N=10,000$, $N^V=5,000$, $\beta=4.62$ month^{-1}, $\alpha=5.16$ month^{-1}, $\mu=6.08$ month^{-1}, $\beta_V=6.69$ month^{-1}, $\alpha_V=2.90$ month^{-1}. (For interpretation of the references to colour in this figure legend, the reader is referred to the web version of this article.)

2.2. Instantaneous epidemic risk (IER)

2.2.1. SIR model

For the SIR model, we consider the IER for a scenario in which a single infectious individual arrives in the population at time $t = t_0$. The IER is given by

$$\text{IER} = 1 - \frac{\mu(t_0)}{\beta(t_0)}, \tag{5}$$

whenever the instantaneous reproduction number at the time of pathogen introduction $\frac{\beta(t_0)}{\mu(t_0)} > 1$ (otherwise the IER is zero). The IER is derived by assuming that infections occur according to a branching process (Text S2). This expression is commonly used to assess epidemic risks in the context of models in which the values of the parameters determining transmission do not change in time, in which case the IER is simply the standard estimate for the probability of a major epidemic starting from a single infectious case (i.e. the IER is $1 - \frac{1}{R_0}$) (Althaus et al., 2015; Thompson et al., 2020a).

2.2.2. Host-vector model

For the host-vector model, we consider the IER for a scenario in which a single exposed host arrives in the population at time $t = t_0$. All other hosts and all vectors are assumed to be susceptible. In this case, the IER is given by

$$\text{IER} = \frac{R^{HV}(t_0)\rho(t_0)R^{VH}(t_0) - 1}{R^{HV}(t_0)\rho(t_0)R^{VH}(t_0) + R^{VH}(t_0)}, \tag{6}$$

whenever $R^{HV}(t_0)\rho(t_0)R^{VH}(t_0) > 1$ (otherwise the IER is zero), as derived in Text S2. In this expression, $R^{HV}(t_0) = \frac{\beta_V(t_0)N^V}{N\mu(t_0)}$ represents the expected number of vectors acquiring the pathogen from a single infectious host in an otherwise susceptible population of hosts and vectors at time $t = t_0$, assuming that the parameters governing transmission are unchanged after time $t = t_0$. Similarly, $R^{VH}(t_0) = \frac{\beta(t_0)}{\delta(t_0)}$ represents the expected number of hosts infected by a single infectious vector in an otherwise susceptible population and $\rho(t_0) = \frac{\alpha_V(t_0)}{\delta(t_0)+\alpha_V(t_0)}$ represents the probability that an exposed vector goes on to become infectious (before dying), in each case assuming that transmission parameters are unchanged after time $t = t_0$.

Eq. (6), and the analogous quantity in which there is no extrinsic incubation period (i.e. $\rho(t_0) = 1$), is often considered in the context of models in which transmission parameters do not vary in time (Lloyd et al., 2007; Thompson et al., 2020a). The IER has also been used previously to assess temporal variations in epidemic risks for host-vector pathogens (Guzzetta et al., 2016a,b; Thompson et al., 2020b).

2.3. Case epidemic risk (CER)

2.3.1. SIR model

To derive the CER for the SIR model, we denote the probability of a major epidemic failing to develop starting from i infectious hosts at time $t = t_0$ by $q_i(t_0)$. If there is a single infectious host at time $t = t_0$, then the probability of a major epidemic failing to develop is denoted by $q_1(t_0)$. We then consider the possible events in the next Δt months (i.e. the time interval $[t_0, t_0 + \Delta t]$, where Δt represents a very short time period so that at most a single event is possible): the probability that an infection event occurs is approximately $\beta(t_0)\Delta t$; the probability that a removal event occurs is approximately $\mu(t_0)\Delta t$; and the probability that no event occurs is approximately $1 - \beta(t_0)\Delta t - \mu(t_0)\Delta t$. Applying the law of total probability therefore gives

$$\begin{aligned} q_1(t_0) = {} & \text{Prob}(\text{infection event occurs in } [t_0, t_0 + \Delta t]) \\ & \times \text{Prob}(\text{no epidemic} \mid \text{infection event occurs in } [t_0, t_0 + \Delta t]) + \text{Prob}(\text{removal event occurs in } [t_0, t_0 + \Delta t]) \\ & \times \text{Prob}(\text{no epidemic} \mid \text{removal event occurs in } [t_0, t_0 + \Delta t]) + \text{Prob}(\text{no event occurs in } [t_0, t_0 + \Delta t]) \\ & \times \text{Prob}(\text{no epidemic} \mid \text{no event occurs in } [t_0, t_0 + \Delta t]), \\ = {} & \beta(t_0)\Delta t q_2(t_0 + \Delta t) + \mu(t_0)\Delta t q_0(t_0 + \Delta t) \\ & + (1 - \beta(t_0)\Delta t - \mu(t_0)\Delta t) q_1(t_0 + \Delta t). \end{aligned} \tag{7}$$

Similarly to our calculation of the IER for the SIR model (Text S2), we assume that infection lineages are independent so that $q_2(t_0 + \Delta t) \approx q_1(t_0 + \Delta t)^2$, and note that $q_0(t_0 + \Delta t) = 1$. The assumption of independent infection lineages is common to any epidemiological branching process model (e.g. Ball and Donnelly, 1995; Britton, 2010; Allen and van den Driessche, 2013). Rearranging Eq. (7) and taking the limit $\Delta t \to 0$ gives

$$\frac{dq_1(t_0)}{dt_0} = -\beta(t_0)q_1(t_0)^2 + (\beta(t_0) + \mu(t_0))q_1(t_0) - \mu(t_0). \tag{8}$$

This equation could be solved numerically with periodic boundary conditions (specifically, since the epidemiological parameters $\beta(t)$ and $\mu(t)$ vary with period 12 months, then we expect $q_1(0) = q_1(12) = q_1(24)$ and so on); this is essentially the extensible approach taken for the host-vector model, as shown in the following subsection. However, for the stochastic SIR model, further analytic progress is possible (Carmona and Gandon, 2020). As shown in Text S3, by solving Eq. (8) an expression for the CER for the stochastic SIR model is derived, given by

$$\text{CER} = 1 - q_1(t_0) = \frac{1}{1 + \int_{t_0}^{\infty} \mu(r)\exp\left(-\int_{t_0}^{r} \beta(s) - \mu(s)ds\right)dr}. \tag{9}$$

2.3.2. Host-vector model

We derive the CER for the host-vector model, considering a scenario in which a single exposed host enters the population at time $t = t_0$. To do this, we denote the probability of a major epidemic failing to develop starting from i exposed hosts, j infectious hosts, k exposed vectors and l infectious vectors in the population at time $t = t_0$ by $q_{ijkl}(t_0)$. Following the method used to derive the CER for the SIR model, considering the possible events in the next Δt months starting from a single exposed host at time $t = t_0$ (where Δt represents a very short time period) gives

$$q_{1000}(t_0) = \alpha(t_0)\Delta t q_{0100}(t_0 + \Delta t) + (1 - \alpha(t_0)\Delta t) q_{1000}(t_0 + \Delta t).$$

As in Eq. (7), this expression is a straightforward application of the law of total probability, where the terms on the right-hand-side represent either the exposed host becoming infectious in the time period $[t_0, t_0 + \Delta t]$ or no event occurring. Rearranging this expression, and taking the limit $\Delta t \to 0$, gives

$$\frac{dq_{1000}(t_0)}{dt_0} = \alpha(t_0)(q_{1000}(t_0) - q_{0100}(t_0)).$$

Similarly, starting instead from a single infected host at time $t = t_0$, gives

$$\begin{aligned} q_{0100}(t_0) = {} & \frac{\beta_V(t_0)N^V}{N}\Delta t q_{0110}(t_0 + \Delta t) + \mu(t_0)\Delta t q_{0000}(t_0 + \Delta t) \\ & + \left(1 - \frac{\beta_V(t_0)N^V}{N}\Delta t - \mu(t_0)\Delta t\right) q_{0100}(t_0 + \Delta t). \end{aligned}$$

Making the assumption that infection lineages are independent (so that $q_{0110}(t_0+\Delta t) = q_{0100}(t_0+\Delta t)q_{0010}(t_0+\Delta t)$), noting that $q_{0000}(t_0+\Delta t) = 1$, then rearranging this expression and taking the limit $\Delta t \to 0$, gives

$$\frac{\mathrm{d}q_{0100}(t_0)}{\mathrm{d}t_0} = -\frac{\beta_V(t_0)N^V}{N}q_{0100}(t_0)q_{0010}(t_0) - \mu(t_0) + \left(\frac{\beta_V(t_0)N^V}{N} + \mu(t_0)\right)q_{0100}(t_0).$$

Instead considering starting from a single exposed vector at time $t = t_0$, or a single infectious vector at time $t = t_0$, allows two similar equations to be derived describing the temporal evolution of $q_{0010}(t_0)$ and $q_{0001}(t_0)$. Denoting the probability of a major epidemic starting from i exposed hosts, j infectious hosts, k exposed vectors and l infectious vectors in the population at time $t = t_0$ by $p_{ijkl}(t_0) = 1 - q_{ijkl}(t_0)$, the following system of equations is obtained:

$$\begin{aligned}
\tfrac{\mathrm{d}p_{1000}(t_0)}{\mathrm{d}t_0} &= \alpha(t_0)(p_{1000}(t_0) - p_{0100}(t_0)),\\
\tfrac{\mathrm{d}p_{0100}(t_0)}{\mathrm{d}t_0} &= \tfrac{\beta_V(t_0)N^V}{N}(p_{0100}(t_0) - 1)p_{0010}(t_0) + \mu(t_0)p_{0100}(t_0),\\
\tfrac{\mathrm{d}p_{0010}(t_0)}{\mathrm{d}t_0} &= -\alpha_V(t_0)p_{0001}(t_0) + (\delta(t_0) + \alpha_V(t_0))p_{0010}(t_0),\\
\tfrac{\mathrm{d}p_{0001}(t_0)}{\mathrm{d}t_0} &= \beta(t_0)p_{1000}(t_0)(p_{0001}(t_0) - 1) + \delta(t_0)p_{0001}(t_0),
\end{aligned} \tag{10}$$

in which the CER is given by $p_{1000}(t_0)$. Since we assume that the parameters governing pathogen transmission vary seasonally (and so are periodic), then the epidemic risk must be periodic, and $p_{1000}(t_0)$, $p_{0100}(t_0)$, $p_{0010}(t_0)$ and $p_{0001}(t_0)$ must also be periodic (each of these variables must take the same values at any values of t_0 that are a multiple of 12 months apart). We therefore solve system of equations (10) numerically on the domain $t_0 \in [0, 24]$ with periodic boundary conditions ($p_{1000}(0) = p_{1000}(24)$, $p_{0100}(0) = p_{0100}(24)$, $p_{0010}(0) = p_{0010}(24)$, $p_{0001}(0) = p_{0001}(24)$) using the Chebfun open-source MATLAB software package (Driscoll et al., 2014).

This approach for estimating the CER can be extended easily for stochastic compartmental models with additional complexity (for models with more infected compartments, further subscripts will be required in the q and p variables). The resulting system of differential equations can then again be solved with periodic boundary conditions using open-source software tools.

3. Results

3.1. SIR model

We first considered the stochastic SIR model, and calculated the IER (Eq. (5); red dotted line in Fig. 1A) and the CER (Eq. (9); blue line in Fig. 1A). While the IER did not match the CER exactly, the IER is a close approximation to the CER for this baseline set of model parameters. We also confirmed the analytic calculation of the CER using model simulations (green circles in Fig. 1B). To approximate the CER in the simulations, the proportion of simulations in which more than 1,000 individuals were ever infected (i.e. $I + R$ exceeded 1,000, which is 10% of the population) was calculated (Fig. 1B-D). This result was not sensitive to the precise threshold value of $I + R$ chosen, as outbreaks either faded out with few infections or large numbers of infections occurred (Fig S2; the simulation results matched the analytic calculation for the range of threshold values of $I + R$ explored except when the threshold was very small).

We then investigated how the difference between the IER and CER varies for outbreaks that invade or fade out at different speeds. Specifically, we considered outbreaks in which the infection and removal rates are changed from $\beta(t)$ and μ to $\sigma\beta(t)$ and $\sigma\mu$, respectively, where the parameter σ governs the magnitude of the transmission parameters relative to the baseline case in Fig. 1. Since the IER depends only on the ratio of the infection and removal rates, it does not depend on σ (unlike the CER). When the value of σ was large, the pathogen invaded or faded out quickly compared to the rates at which environmental conditions were assumed to change. As a result, the IER matched the CER closely (Fig. 2E). However, when instead the value of σ was small, the pathogen either invaded the population or faded out slowly, and so the CER was impacted significantly by changes in environmental conditions over the duration of the initial phase of the outbreak. As a result, the CER and IER no longer matched closely (e.g. Fig. 2A–C). As the value of σ approached zero, the rate at which the pathogen invaded or faded out was so slow that periodicity in environmental conditions did not have an effect on the CER (Fig. 2A). In this case, the CER approaches the standard branching process estimate for the probability of a major epidemic, $1 - 1/R_0$ (see also the asymptotic analysis by Carmona and Gandon (2020)).

The error between the IER and CER, computed as $\frac{\int_0^{12}|\mathrm{CER}(t_0)-\mathrm{IER}(t_0)|\mathrm{d}t_0}{\int_0^{12}\mathrm{CER}(t_0)\mathrm{d}t_0}$, is shown in Fig. 2F as a function of the parameter σ that characterises the speed at which the pathogen either invades the population or fades out.

3.2. Host-vector model

We then extended our analysis to a setting in which the pathogen is transmitted between hosts via vectors and the vector lifespan depends on the temperature at different times of year (Fig. 3A). As described in the Methods, the monthly temperature in Miami was characterised by fitting the expression in Eq. (4) to data using least squares estimation (Fig. 3B), thereby allowing the instantaneous vector lifespan and the corresponding vector mortality rate ($\delta(t)$) to be calculated at different times of year (Fig. 3C).

To isolate the effect of a temporally varying vector lifespan on the probability that an imported case will generate a major epidemic, we assumed that all other parameters governing pathogen transmission in the host-vector model took constant values, and calculated the IER and the CER (Fig. 3D). We also verified that the CER was approximated closely by the analogous quantity calculated using model simulations (green circles in Fig. 3D). For the host-vector model, there were notable differences between the IER and CER. When environmental conditions were instantaneously optimal for vector survival at the time of pathogen introduction (so that the IER is high), then the IER overestimated the CER since conditions in future were due to change to a state that was less favourable for vector survival. In contrast, when environmental conditions were instantaneously least suitable for vector survival, then the IER instead underestimated the CER since environmental conditions improved (from the viewpoint of the vector) shortly after introduction.

Since, over the course of a year, the temperature sometimes exceeded the optimal temperature for vector survival (*cf.* Fig. 3A-B), the hottest period of the year did not correspond to the highest value of the IER. Instead, the IER is seen to peak twice per year when the temperature is optimal for vector survival. However, the true probability of pathogen invasion starting from a single infectious host entering the population at time t (i.e. the CER) did not display these biannual peaks (blue line and green circles in Fig. 3D).

4. Discussion

Changes in environmental conditions have a substantial impact on the dynamics of infectious disease outbreaks. Here, we have focused on the earliest stages of outbreaks and estimating the probability that cases introduced at different times of year will lead to major epidemics with large numbers of infections. We defined two quantities: the IER and the CER. While this terminology has not been used previously, as described in the introduction the IER and CER have both been used to assess epidemic risks in different studies. For practical assessments of epidemic risks, it is important to understand when it is necessary to use the more complex CER rather than the easy-to-calculate IER, and to provide methods for calculating those quantities that can be used with stochastic compartmental models of seasonal epidemics with arbitrary complexity.

We found that, when a pathogen establishes in a host population or fades out quickly, the IER and CER take similar values. In those cases, the IER can be used to approximate the CER. However, when the pathogen invades or fades out more slowly, the IER should not be used to estimate the epidemic risk. We compared the IER and CER for a simple epidemiological model describing a pathogen that is transmitted directly from host to host (the stochastic SIR model – Figs. 1-2), as well as for a more complex host-vector model in which the vector lifespan is assumed to vary temporally (Fig. 3). In the host-vector model, we considered realistic seasonal changes in the vector lifespan by combining a previously inferred temperature-vector lifespan relationship for *Aedes aegypti* mosquitoes (Yang et al., 2009) with monthly temperature data from Miami (National Oceanic and Atmospheric Administration, 2020) (Fig. 3A-B). While the purpose of this study was not to develop a detailed scenario-specific transmission model, we used temperature data from Miami since this is a location that has suitable conditions for vector survival yet currently experiences only limited transmission of globally important vector-borne pathogens such as the dengue virus. As a result, assessing the epidemic risk in locations like Miami is a key public health question (Robert et al., 2016). We observed the potential for biannual peaks in the IER when temperatures are "higher than optimal" for transmission in summer (Fig. 3D). However, biannual peaks were not observed in the CER, which was highest each year before optimal transmission conditions occurred.

Previous assessments of epidemic risks have often involved assuming that the values of transmission parameters do not vary temporally (Daon et al., 2020; Thompson et al., 2016, 2020a; Lovell-Read et al., 2021; Althaus et al., 2015; Thompson, 2020; Hellewell et al., 2020). For example, during the 2014–16 Ebola epidemic in West Africa, the risk that a case introduced to Nigeria would lead to a substantial local epidemic was calculated based on the estimated basic reproduction number (Althaus et al., 2015), and similar analyses were conducted at the start of the COVID-19 pandemic to assess the epidemic risk outside China (Anzai et al., 2020; Thompson, 2020). In other studies (e.g. Guzzetta et al., 2016a,b; Thompson et al., 2020b), temporal changes in environmental conditions have been accounted for explicitly in the underlying models, yet epidemic risks have then been calculated by assuming implicitly that environmental conditions are fixed at the time when the pathogen is introduced into the population (i.e. the IER has been used). For example, Guzzetta et al. (2016b) considered a model of Zika virus transmission dynamics in which parameter values are temperature-dependent, and then used the IER to estimate the risk of local epidemics. This indicates the need for additional research into when precisely the IER can be used to approximate the CER in applied epidemiological modelling studies, as well as flexible methods for calculating the CER easily for different epidemiological models.

As described in the Introduction, calculation of invasion or extinction probabilities in ecological and epidemiological models has a long history, dating back at least as far as the 1940s (Kendall, 1948). More recently, Carmona and Gandon (2020) considered epidemic probabilities in seasonal environments, demonstrating a so-called "winter is coming" effect: if a pathogen enters a population when conditions are favourable for transmission, but conditions deteriorate in the near future, then pathogen invasion is unlikely. In that setting, the IER is high but the CER is low. While those authors effectively demonstrate that the IER and CER may not always match, in addition to the new terminology that we have devised there are three key differences in the research that we have presented here. First, we provide a simple approach for calculating the CER (see calculation of the CER for the host-vector model) that can be extended straightforwardly for more complex epidemiological models and scenarios, allowing widely available software tools for solving differential equations to be used to assess CERs in periodic environments. Second, we confirm that calculations of the CER are matched by approximations using stochastic simulations for a host-vector model. Third, we show how our approach can be applied directly to data describing seasonal changes in environmental conditions (specifically, we use temperature data from Miami).

Going forwards, practical use of either the IER or CER may require the underlying epidemiological models to be extended to include additional realism. For example, we assumed that the only temperature-dependent variable in the host-vector model was the vector lifespan. While this parameter is sensitive to changes in environmental conditions (Fig. 3A), host-vector models could in theory be extended to consider the effect of a range of environmental factors on different ecological and epidemiological variables. We note that changes in environmental variables could have complex and competing effects on epidemic risks. For example, an increase in the temperature could be beneficial for vector survival (Fig. 3A), but high temperatures may be detrimental for pathogen survival (Lowen and Steel, 2014; Morris et al., 2021). Whichever biological or epidemiological features are included in the underlying compartmental model, our approaches for calculating the IER and CER can be adapted easily.

We considered scenarios in which major epidemics can be differentiated straightforwardly from minor outbreaks. The final size distribution was therefore bimodal: simulated outbreaks were either major epidemics, in which large numbers of infections occurred (Fig. 1C-D), or minor outbreaks in which few individuals were ever infected. The epidemic risk then corresponded to the proportion of simulated outbreaks that were major epidemics. However, there is not always a clear difference between minor outbreaks and major epidemics. For example, for standard epidemic models with parameter values that are not time-dependent, if the basic reproduction number is close to one then the final size distribution is no longer bimodal (Kendall, 1956; Nasell, 1995; Britton, 2010). When outbreaks cannot be partitioned obviously into minor outbreaks and major epidemics, careful consideration of exactly what constitutes a major epidemic is necessary (Thompson et al., 2020a), and the epidemic risk can then be calculated using model simulations (in a similar fashion to the green circles in Figs. 1B and 3D).

Our study involved estimating the epidemic risk when a pathogen is introduced into a new host population. We assumed that the values of the parameters governing transmission were known. As such, our methods are particularly well-suited to scenarios in which the epidemiology of the outbreak-causing pathogen is

understood clearly, but where the pathogen causes either sporadic outbreaks or is transported to new locations. Ebola outbreaks, for example, occur every few years with no transmission in between, and the risk of major Ebola epidemics is of widespread interest. A highly relevant host-vector pathogen is dengue virus, which is regularly imported to locations worldwide by travellers, yet only sometimes leads to sustained local transmission. Future work could involve combining the IER and CER with estimates of the probability of introduction (Daon et al., 2020), which may itself vary seasonally. While we focused on varying environmental conditions, our approach could be applied to estimate epidemic risks that change because of other factors. Real-time calculation of the CER requires future changes in transmission conditions to vary predictably. While this might not always occur, relevant examples where transmissibility may change at predictable timepoints include childhood diseases. For pathogens infecting children, there may be an increased opportunity for transmission during school terms when children have large numbers of contacts, and a reduced opportunity for transmission in school holidays. The modelling framework proposed here could be used to investigate how these contact patterns affect epidemic risks.

5. Conclusion

In summary, we have defined two quantities – the IER and the CER – for estimating the risk from emerging pathogens when environmental conditions vary seasonally. We have shown how the IER and CER can be assessed, including providing a straightforward method for calculating the CER numerically using existing software packages. Using this approach to inform disease surveillance or control strategies requires the underlying models to be conditioned to the specific pathogen, host population and environment under consideration.

We have demonstrated how the difference between the IER and CER varies for outbreaks of different speeds, with a large disparity between these quantities when the pathogen either invades the population or fades out slowly compared to changes in environmental conditions. While the IER can sometimes be a good proxy for the CER, and the IER can be calculated when future changes in transmission are unknown, we conclude that the CER is the main quantity that should be used in studies of seasonal epidemic risks. We hope that our research will facilitate accurate epidemic risk calculations in future applied epidemiological modelling studies.

Funding

This research was funded by an undergraduate summer research bursary from the University of Oxford Mathematical Institute (JB) and an EPSRC Excellence Award (WSH). It was also funded by the EPSRC through the Mathematics for Real-World Systems CDT (ARK, RNT; grant number EP/S022244/1). The collaboration between SI and RNT was funded by an International Exchange grant from the Royal Society and a Computer Science small grant from the London Mathematical Society.

CRediT authorship contribution statement

A.R. Kaye: Investigation, Writing – original draft, Writing – review & editing. **W.S. Hart:** Supervision, Writing – review & editing. **J. Bromiley:** Funding acquisition, Investigation. **S. Iwami:** Conceptualization. **R.N. Thompson:** Funding acquisition, Conceptualization, Investigation, Supervision, Writing – original draft, Writing – review & editing.

Declaration of Competing Interest

The authors declare that they have no known competing financial interests or personal relationships that could have appeared to influence the work reported in this paper.

Acknowledgements

Thanks to Francesca Lovell-Read, Sumali Bajaj and Nik Cunniffe for helpful discussions about this work.

Appendix A. Supplementary data

Supplementary data to this article can be found online at https://doi.org/10.1016/j.jtbi.2022.111195.

References

Abbott, S., Hellewell, J., Thompson, R.N., Sherratt, K., Gibbs, H.P., Bosse, N.I., et al., 2020. Estimating the time-varying reproduction number of SARS-CoV-2 using national and subnational case counts. Wellcome Open Res. 5, 112.
Allen, L.J.S., van den Driessche, P., 2013. Relations between deterministic and stochastic thresholds for disease extinction in continuous- and discrete-time infectious disease models. Math. Biosci. 243, 99–108.
Althaus, C.L., Low, N., Musa, E.O., Shuaib, F., Gsteiger, 2015. Ebola virus disease outbreak in Nigeria: transmission dynamics and rapid control. Epidemics 11, 80–84.
Anzai, A., Kobayashi, T., Linton, N.M., Kinoshita, R., Hayashi, K., Suzuki, A., et al., 2020. Assessing the impact of reduced travel on exportation dynamics of novel coronavirus infection (COVID-19). J. Clin. Med. 9, 601.
Bacaër, N., 2020a. Deux modèles de population dans un environnement périodique lent ou rapide. J. Math. Biol. 80, 1021–1037.
Bacaër, N., 2020b. Sur la probabilité d'extinction d'une population dans un environnement périodique lent. Revue Africaine de la Recherche en Informatique et Mathématiques Appliquées 32, 81–95.
Bacaër, N., Ait Dads, E.H., 2014. On the probability of extinction in a periodic environment. J. Math. Biol. 68, 533–548.
Bacaër, N., Ed-Darraz, A., 2014. On linear birth-and-death processes in a random environment. J. Math. Biol. 69, 73–90.
Ball, F.G., 1983. The threshold behaviour of epidemic models. J. Appl. Probability 20, 227–241.
Ball, F., Donnelly, P., 1995. Strong approximations for epidemic models. Theory Probability Appl. 55, 1–21.
Borremans, B., Faust, C., Manlove, K.R., Sokolow, S.H., Lloyd-Smith, J.O., 2019. Cross-species pathogen spillover across ecosystem boundaries: Mechanisms and theory. Philos. Trans. R. Soc. B 374, 20180344.
Britton, T., 2010. Stochastic epidemic models: A survey. Math. Biosci. 225, 24–35.
Carmona, P., Gandon, S., 2020. Winter is coming: Pathogen emergence in seasonal environments. PLoS Comput. Biol. 16, e1007954.
Cori, A., Ferguson, N.M., Fraser, C., Cauchemez, S., 2013. A new framework and software to estimate time-varying reproduction numbers during epidemics. Am. J. Epidemiol. 178, 1505–1512.
Craft, M.E., Beyer, H.L., Haydon, D.T., 2013. Estimating the probability of a major outbreak from the timing of early cases: an indeterminate problem? PLoS ONE 8, e57878.
Daon, Y., Thompson, R.N., Obolski, U., 2020. Estimating COVID-19 outbreak risk through air travel. J. Travel Med. 27, taaa093.
Dowell, S.F., 2001. Seasonal variation in host susceptibility and cycles of certain infectious diseases. Emerging Infect. Dis. 7, 369–374.
Driscoll, T.A., Hale, N., Trefethen, L.N., 2014. Chebfun Guide. Pafnuty Publications, Oxford.
Gillespie, D.T., 1977. Exact stochastic simulation of coupled chemical reactions. J. Phys. Chem. 8, 2340–2361.
Gostic, K.M., McGough, L., Baskerville, E., Abbott, S., Joshi, K., Tedijanto, C., et al., 2020. Practical considerations for measuring the effective reproductive number, R_t. PLoS Comput. Biol. 16, e1008409.
Grassly, N.C., Fraser, C., 2006. Seasonal infectious disease epidemiology. Proceed. R. Soc. B 273, 2541–2550.
Guzzetta, G., Montarsi, F., Baldacchino, F.A., Metz, M., Capelli, G., Rizzoli, A., et al., 2016a. Potential risk of dengue and Chikungunya outbreaks in Northern Italy based on a population model of Aedes albopictus (Diptera: Culicidae). PLoS Negl. Trop. Dis. 10, e0004762.
Guzzetta, G., Poletti, P., Montarsi, F., Baldacchino, F., Capelli, G., Rizzoli, A., et al., 2016b. Assessing the potential risk of Zika virus epidemics in temperate areas with established Aedes albopictus populations. Eurosurveillance 21, 30199.
Hellewell, J., Abbott, S., Gimma, A., Bosse, N.I., Jarvis, C.I., Russell, T.W., et al., 2020. Feasibility of controlling COVID-19 outbreaks by isolation of cases and contacts. Lancet Global Health. 8, e488–e496.

Kendall, D.G., 1948. On the generalized 'birth-and-death' process. Ann. Math. Stat. 19, 1–15.
Kendall, D.G., 1956. Deterministic and stochastic models in closed populations. Proc 3rd Berkeley Symp. Math. Stat. Prob. 4, 149–165.
Kucharski, A.J., Funk, S., Eggo, R.M., Mallet, H.P., Edmunds, W.J., Nilles, E.J., 2016. Transmission dynamics of Zika virus in island populations: A modelling analysis of the 2013–14 French Polynesia outbreak. PLoS Negl. Trop. Dis. 10, e0004726.
Lloyd, A.L., Zhang, J., Root, A.M., 2007. Stochasticity and heterogeneity in host-vector models. J. R. Soc. Interface 4, 851–863.
Lloyd-Smith, J.O., George, D., Pepin, K.M., Pitzer, V.E., Pulliam, J.R.C., Dobson, A.P., et al., 2009. Epidemic dynamics at the human-animal interface. Science 362, 1362–1367.
Lovell-Read, F.A., Funk, S., Obolski, U., Donnelly, C.A., Thompson, R.N., 2021. Interventions targeting non-symptomatic cases can be important to prevent local outbreaks: SARS-CoV-2 as a case study. J. R. Soc. Interface 18, 20201014.
Lowen, A.C., Steel, J., 2014. Roles of humidity and temperature in shaping influenza seasonality. J. Virol. 88, 7692–7695.
Mastin, A.J., Gottwald, T.R., van den Bosch, F., Cunniffe, N.J., Parnell, S.R., 2020. Optimising risk-based surveillance for early detection of invasive plant pathogens. PLoS Biol. 18, e3000863.
Moriyama, M., Ichinohe, T., 2019. High ambient temperature dampens adaptive immune responses to influenza A virus infection. Proc. Natl. Acad. Sci. USA 116, 3118–3125.
Morris, D.H., Yinda, K.C., Gamble, A., Rossine, F.W., Huang, Q., Bushmaker, T., et al., 2021. Mechanistic theory predicts the effects of temperature and humidity on inactivation of SARS-CoV-2 and other enveloped viruses. eLife 10, e65902.
Nandi, A., Allen, L.J.S., 2021. Probability of a zoonotic spillover with seasonal variation. Infect. Dis. Modell. 6, 514–531.
Nasell, I., 1995. The threshold concept in stochastic epidemic and endemic models. In: Mollison, D. (Ed.), Epidemic models: their structure and relation to data. Cambridge University Press.
Nipa, K.F., Allen, L.J.S., 2020. Disease emergence in multi-patch stochastic epidemic models with demographic and seasonal variability. Bull. Math. Biol. 82, 152.
National Oceanic and Atmospheric Administration. Climate Data Online Search [Internet]. 2020 [cited 2020 Sep 10]. Available from: https://www.ncdc.noaa.gov/cdo-web/search.
Plowright, R.K., Parrish, C.R., McCallum, H., Hudson, P.J., Ko, A.I., Graham, A.L., et al., 2017. Pathways to zoonotic spillover. Nat. Rev. Microbiol. 15, 502–510.
Robert, M.A., Christofferson, R.C., Silva, N.J.B., Vasquez, C., Mores, C.N., Wearing, H.J., 2016. Modeling mosquito-borne disease spread in U.S. urbanized areas: The case of dengue in Miami. PLoS ONE 11, e0161365.
Rowley, W.A., Graham, C.L., 1968. The effect of temperature and relative humidity on the flight performance of female Aedes aegypti. J. Insect Physiol. 14, 1251–1257.
Shaman, J., Kohn, M., 2009. Absolute humidity modulates influenza survival, transmission, and seasonality. Proc. Natl. Acad. Sci. USA 106, 3243–3248.
Tang, J.W., 2009. The effect of environmental parameters on the survival of airborne infectious agents. J. R. Soc. Interface 6, S737–S746.
Thanh, V.H., Priami, C., 2015. Simulation of biochemical reactions with time-dependent rates by the rejection-based algorithm. J. Chem. Phys. 143, 054104.
Thompson, R.N., 2020. Novel coronavirus outbreak in Wuhan, China, 2020: Intense surveillance is vital for preventing sustained transmission in new locations. J. Clin. Med. 9, 498.
Thompson, R.N., Gilligan, C.A., Cunniffe, N.J., 2016. Detecting presymptomatic infection is necessary to forecast major epidemics in the earliest stages of infectious disease outbreaks. PLoS Comput. Biol. 12, e1004836.
Thompson, R.N., Gilligan, C.A., Cunniffe, N.J., 2020a. Will an outbreak exceed available resources for control? Estimating the risk from invading pathogens using practical definitions of a severe epidemic. J. R. Soc. Interface 17, 20200690.
Thompson, R.N., Thompson, M.J., Hurrell, J.W., Sun, L., Obolski, U., 2020b. Assessing the threat of major outbreaks of vector-borne diseases under a changing climate. Astrophys. Space Sci. Proceed. 57.
Thompson, R.N., Stockwin, J.E., Van, G.RD., Polonsky, J.A., Kamvar, Z.N., Demarsh, P.A., et al., 2019a. Improved inference of time-varying reproduction numbers during infectious disease outbreaks. Epidemics 19, 100356.
Thompson, R.N., Thompson, C., Pelerman, O., Gupta, S., Obolski, U., 2019b. Increased frequency of travel in the presence of cross-immunity may act to decrease the chance of a global pandemic. Philos. Trans. R. Soc. B 374, 20180274.
White, L.F., Moser, C.B., Thompson, R.N., Pagano, M., 2020. Statistical estimation of the reproductive number from case notification data. Am. J. Epidemiol., kwaa211
Wilson, M.E., 1995. Travel and the emergence of infectious diseases. Emerg. Infect. Dis. 1, 39–46.
Yang, H.M., Macoris, M.L.G., Galvani, K.C., Andrighetti, M.T.M., Wanderley, D.M.V., 2009. Assessing the effects of temperature on the population of Aedes aegypti, the vector of dengue. Epidemiol. Infect. 137, 1188–1202.